Modeling Biochemical Networks: A Cellular-Automata Approach

by **Lemont B. Kier**, **Danail Bonchev***, and **Gregory A. Buck**

Center for the Study of Biological Complexity, Virginia Commonwealth University, P.O. Box 842030, Richmond, VA 23284-2030, USA
(phone: +1-804-827-7375, +1-804-827-0026; e-mail: lbkier@vcu.edu, dgbonchev@vcu.edu, gabuck@vcu.edu)

The potential of the cellular-automata (CA) method for modeling biological networks is demonstrated for the mitogen-activated protein kinase (MAPK) signaling cascade. The models derived reproduced the high signal amplification through the cascade and the deviation of the cascade enzymes from the *Michaelis–Menten* kinetics, evidencing cooperativity effects. The patterns of pathway change upon varying substrate concentrations and enzyme efficiencies were identified and used to show the ways for controlling pathway processes. Guidance in the selection of enzyme inhibition targets with minimum side effects is one outcome of the study.

1. Introduction. – Since its introduction 50 years ago, cellular automata (CA) have been used to conduct studies of various dynamical systems [1]. Of interest to us is the emerging role played by CA in the area of dynamic biological systems. Some applications to the modeling of physical systems, such as kinetic and thermodynamic control of chemical reactions, have been reported [2]. These studies point the way to the application of CA to encode the outcomes of the emerging properties in dynamic biochemical systems resulting from changes due to concentration alteration.

Biological cell function is related to the interplay of macromolecules, mostly proteins that function as enzymes, and substrates. The antecedents of these proteins are the genes that program their creation. The totality of these molecules can be displayed as networks to reveal the functional relationships among them. A prominent direction of research today is to identify the 'ingredients' that comprise the structural details of these networks. The next step is to attempt to model a fragment of the network that has a demonstrable biological function, the ultimate goal being the modeling of the entire network.

Dynamic evolutionary networks have recently been recognized as a universal approach to complex systems, ranging from quantum gravity to biological cells and organisms, ecosystems, social groups, and market economy. The network approach is a non-reductionist approach enabling analysis of the systems as a whole, which makes it an ideal tool for system biology. Network topology is generally used in characterizing networks, focusing on their connectivity, neighborhood, and distance relationships. Network complexity has also been recently quantitatively characterized [3]. This abundance of cellular-network data – produced by microarrays, two-dimensional gel chromatography, mass spectroscopy, and other techniques – brings about another dimension of the network approach, allowing the tracing of the continuous changes of

network species and their interactions. The large size of the metabolic, protein, and gene regulatory networks is a serious challenge for the traditional methods based on dynamic modeling. It is the purpose of this study to outline the potential of CA as a basic method for the dynamic modeling of networks having biological and medical applications. Some preliminary work on the CA modeling of enzymatic reactions has already been published [4–6]. However, it has been limited to the simplest cases of linear chains of reactions and the feed-forward mechanism. In this work, we apply the CA technique to an important signaling pathway characterized by considerable complexity.

2. Methodology. – 2.1. *Abbreviations.* For the sake of presentation compactness, particularly that of the figures and equations, a number of abbreviations have been used. They are collected in *Table 1*.

Table 1. *List of Abbreviations Used*

Symbol	Meaning
CA	Cellular automata
2-D	Two-dimensional
P_c	Transition probability (probability of an ES pair of cells turning into an EP pair of cells); also called *enzyme efficiency*
ES	Enzyme–substrate complex
EP	Enzyme–product complex
E1 and E2	Enzymes catalyzing the forward and reverse reactions of MAPKKK activation and deactivation (see *Fig. 1*)
E3	Enzyme catalyzing the dephosphorylation of MAPKK-PP and MAPKK-P (see *Fig. 1*)
E4	Enzyme catalyzing the dephosphorylation of MAPK-PP and MAPK-P (see *Fig. 1*)
F = MAPK	Mitogen-activated protein kinase (also known as ERK, extracellular signal-regulated kinase)
C = MAPKK	Mitogen-activated protein kinase kinase (also known as ERKP, phosphorylated ERK)
A = MAPKKK	Mitogen-activated protein kinase kinase kinase (also known as RAF, a serine/threonine protein kinase)
B = MAPKKK*	Activated MAPKKK (also known as RAF*)
D = MAPKK-P	Monophosphorylated MAPKK (also known as MEKP, a protein kinase that phosphorylates the ERK gene product)
E = MAPKK-PP	Diphosphorylated MAPKK
G = MAPK-P	Monophosphorylated MAPK
H = MAPK-PP	Diphosphorylated MAPK

2.2. *Cellular Automata.* Cellular automata (CA) are dynamic systems that are discrete in space, time, and state, and whose behavior is specified completely by rules governing local relationships. As shown by *Toffoli* [7], CA are an alternative, rather than an approximation, of differential equations in modeling physics and chemistry. The 2-D CA models are built on a grid of usually square spaces called *cells.* The grid of cells may vary depending on the problem to examine. Each cell, has four adjoining neighbors, *j*, and four extended neighbors beyond *j*. This is called an extended *von Neumann* neighborhood. The CA dynamic simulations are run on the surface of a torus to eliminate a boundary condition. Thus, movement past an edge puts the substance at the opposite face.

Each cell is assigned a state governing whether it is empty or occupied by an enzyme, a substrate, or a product in our model. The contents of a cell may break away from an occupied neighboring cell or move to join a neighboring cell that is occupied. These trajectories are assigned as probabilistic rules at the beginning of the dynamics to reflect an anticipated relationship among the ingredients in the system. The rules are then applied to each cell at random, until all cells have computed their states and trajectories. This represents one iteration of time. The rules are applied uniformly to each cell of the same state. The initial state of the system is random and, thus, does not determine subsequent configurations at any iteration. The same set of rules does not yield the same configurations, except in some average sense. The configurations after many iterations reach a collective organization that possesses relative constancy in appearance and in reportable counts of cells, called *attributes*. These are the emergent characteristics of a complex system.

Our 2-D CA model is composed of a 100×100 grid. The probabilities of joining and breaking away are assumed to be equal to unity. Each of the models was obtained as the average of 50 runs, each of which included 5000 to 15000 iterations, a number sufficiently large to enable reproducing the steady state of the set of reactions examined (see, *Fig. 2* below). Focusing more on the final result of the iterations than on the temporal changes, our model is a *spatial* one. A network to be studied is represented by groups of CA cells, each group representing one of the network species, an enzyme, a substrate, and a product. The number of cells in each group reflects the relative concentrations of each network ingredient. Each group of cells moves about freely in the grid. They may encounter each other, but this has generally no consequence. The only encounters that have a consequence are those between a specific substrate and a specific enzyme. When such an encounter occurs, an enzyme–substrate complex is modeled. This complex has an assigned probability of changing to a new complex (enzymatic product). Following this, there is a probability assigned for the separation of these two species.

2.3. *The Rules.* Probability rules govern the movement, joining, and breaking of cell species of all kinds. Each species type X is characterized by a set of parameters governing its relationship to itself and to all other cell species of type Y. The joining parameters, $J(\mathrm{XX})$ and $J(\mathrm{XY})$, determine the extent of cell X moving toward another cell X or Y in a *von Neumann* neighborhood. The breaking parameters $P_{\mathrm{B}}(\mathrm{XX})$ and $P_{\mathrm{B}}(\mathrm{XY})$ determine the extent of disruption of adjacent cells occupied with like or unlike ingredients. The movement probability, P_{m}, determines the extent of any movement. Thus, for an enzyme cell, $P_{\mathrm{M}} = 0$ would designate a stationary enzyme. The CA model selected is asynchronous. Cells compute their states one at a time. In our study, all three types of probabilities were assumed equal to unity: $P_{\mathrm{J}} = P_{\mathrm{B}} = P_{\mathrm{M}} = 1$. This means that all cells may interact, join, and break apart with equal probability. Only the cells involved in a specific state change, *i.e.*, enzyme–substrate (ES) $\rightarrow$ enzyme–product (EP), are endowed with a state-change-probability rule, defined by the transition probability P_{c}, which describes the probability of an ES pair of cells changing to an EP pair of cells. It may be regarded as a measure for enzyme activity or efficiency [8], terms that will be interchangeably used in this paper. The collection of rules associated with a network species represents, thus, a profile of the structure of that species and its relationship with other species, within our definition of a molecular

system. By systematically varying the rules, we can develop a profile of configurations reflecting the influences of different structures. We will follow the general method used by *Kier* and *Cheng* [5] in setting up a CA model of enzyme activity.

a)

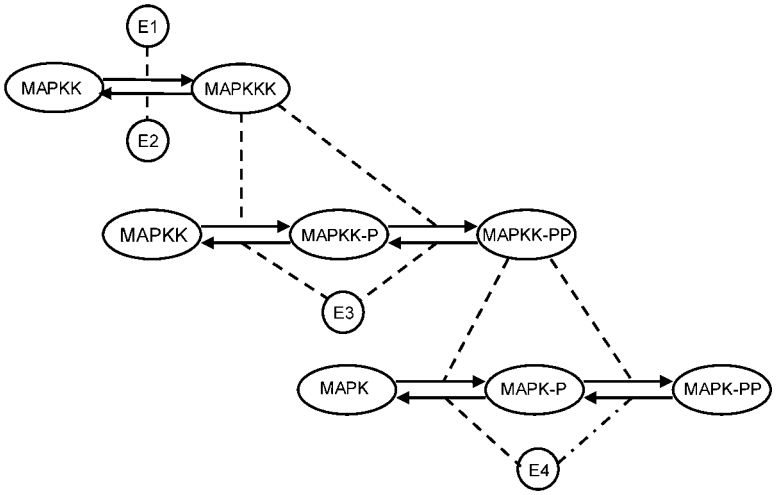

b)

A + E1 → AE1 → BE1 → B + E1

B + E2 → BE2 → AE2 → A + E2

C + B → CB → DB → D + B

D + B → DB → EB → E + B

D + E3 → DE3 → CE3 → C + E3

E + E3 → EE3 → DE3 → D + E3

F + E → EF → EG → G + E

G + E → EG → EH → H + E

G + E4 → GE4 → FE4 → F + E4

H + E4 → HE4 → GE4 → G + E4

Fig. 1. a) *The MAPK signaling cascade* [9]. Dashed lines indicate catalyst action. b) *The corresponding set of cascade enzymatic reactions.* A = MAPKKK, B = MAPKKK*, C = MAPKK, D = MAPKK-P, E = MAPKK-PP, F = MAPK, G = MAPK-P, and H = MAPK-PP (see also *Table 1*). E3 and E4 are the MAPKK- and MAPK-proteases, respectively, and the hypothetical enzymes E1 and E2 affect the reactions of MAPKKK activation and deactivation. The product B of the first reaction is an enzyme that activates the second row of forward reactions in the cascade. At its turn, the product of these phosphorylation reactions activates the forward reactions in the third cascade row.

3. The CA Modeling of the Mitogen-Activated Protein Kinase Signaling Pathway. We have begun our analysis of cell networks with the mitogen-activated protein kinase (MAPK) cascade as an example of importance, studied recently by different numerical methods (differential equations, stochastic approaches, *etc.*) based on reaction-rate equations [9–16]. This is a signaling pathway in which signals from the plasma membrane are relayed to targets in the cytoplasm and nucleus. Considerable progress has been achieved during the last decade in elucidating the detailed molecular mechanism of this pathway [12]. Aiming to test the applicability of the CA method to pathways and networks, we limited our study to the major cascade part of the MAPK pathway, which has been incorporated in all biochemical models proposed so far. The cascade is shown schematically in *Fig. 1,a*, as given by *Huang* and *Ferell* [9]. The set of the MAPK cascade biochemical reactions implies the detailed reaction mechanism shown in *Fig. 1,b*.

The CA model is built from the above reaction mechanisms. The three substrates MAPKKK, MAPKK, and MAPK, and the four enzymes involved have some prescribed initial concentrations (assigned a number of CA cells). We have systematically altered the initial concentrations of the above substrates, as well as the efficiencies of the enzymes. The basic variable was the concentration of MAPKKK, which was varied within a 25-fold range from 20 to 500 cells. This matches the 25-fold range of variation of E1 used as an initial stimulus in the original study [9]. The concentrations of MAPKK and MAPK were kept constant (500 or 250 cells) in most of the models. The four enzymes, denoted by E1, E2, E3, and E4, were represented in the CA grid by 50 cells each. In one series of models, we kept the MAPKKK initial concentration equal to 50 cells, set the transition probabilities of three of the enzymes

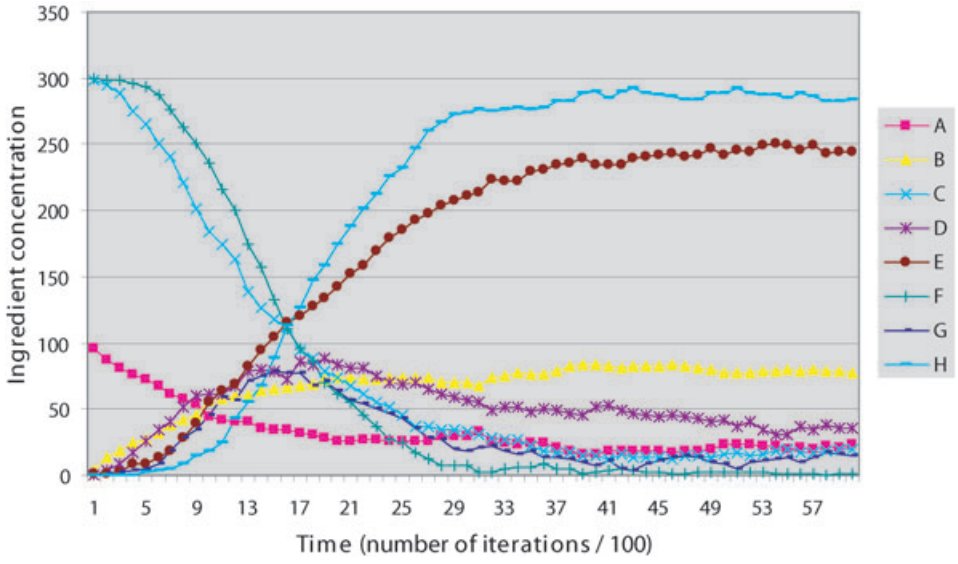

Fig. 2. *Temporal change in ingredient concentrations from* t = *0 to the steady state reached for less than 15000 cellular-automata iterations* (see *Fig. 1,b* for the full names of the ingredients A–H)

to $P_c = 0.1$, and varied the probability of the fourth enzyme between 0% and 100%. In another series, *all* enzyme transition probabilities were kept constant ($P_c = 0.1$), whereas the concentrations of substrates were varied. In a third series, both substrate concentrations and enzyme efficiencies were varied. Recorded were the variations in the steady-state concentrations of the three substrates MAPKKK, MAPKK, and MAPK, and those of the products MAPKKK*, MAPKK-P, MAPKK-PP, MAPK-P, and MAPK-PP. An illustration of the system time changes from $t = 0$ up to reaching a steady state after a certain number of CA iterations is shown in *Fig. 2*. The parameter values used were as follows. Initial concentrations: $[A]_0 = 100$, $[C]_0 = [F]_0 = 300$; $[E1]_0 = 50$, $[E2]_0 = [E3]_0 = [E4]_0 = 10$ cells; enzyme transition probabilities: $P_c = 0.1$.

The immediate question to answer in analyzing a signaling pathway is whether the model reproduces the amplification of the signal through the cascade. The quantitative aspects of signal amplification are also important in the examination of the overall cascade sensitivity to a variety of initial conditions. It was particularly important to show that CA models can reproduce the sigmoidal character of the concentration change of the basic MAPK cascade species. In addition, as a CA model for a future, more-general analysis of networks and pathways, this study was also focused on the patterns of substrate and product variations, and the ways to control these patterns toward a desirable outcome. The change in substrate concentration predetermines the outcome of the *reversible* reactions. The change in enzyme concentration affects only the rate at which the reaction reaches the equilibrium state. However, in *non-equilibrium* reactions, which frequently occur in biochemistry, different enzyme concentrations produce different steady states, thus influencing the degree of conversion of substrates into products. The goal of this work was to show that the CA method provides an adequate answer to all these questions.

4. Results and Discussion. – 4.1. *Modeling Enzyme Activity.* Upgrading or downgrading enzyme activities are one of the typical ways cells react to stress and interactions with pathogens. We studied systematically the variations of one of the four enzymes E1 to E4 at constant concentrations of the substrates MAPKKK, MAPKK, and MAPK, assuming constant efficiency of the other three enzymes. This type of pathway is illustrated in *Fig. 3* with the variation of the MAPKK protease (E3 in *Fig. 1*), which reverses the two-step reaction of MAPKK phosphorylation. It is shown that the concentration of both the MAPKK and MAPK diphosphates (E and H, resp., in *Fig. 3*) passes through a maximum near a relatively low enzyme-transition probability ($P \approx 0.02$). At the maximum point, the concentration of MAPK-PP reaches over 80% of its possible value, whereas that of MAPKK-PP is slightly over 50%. This shows the potential for a strong influence on the concentrations of the two diphosphates in the MAPK cascade, and, thus, on the amplification of the cascade signal, by inhibiting the MAPKK protease. In contrast, the level of steady-state concentrations of the two monophosphates (D and G in *Fig. 2*) is not sensitive to the activity of the enzyme modeled, except for the extreme case of very strong inhibition ($P \rightarrow 0.001$).

More results from the modeling of the variations in the four enzyme efficiencies are presented in *Table 2*. They illustrate the possibility to use the identified patterns for biochemical control of the MAPK cascade pathway. Similar patterns have been

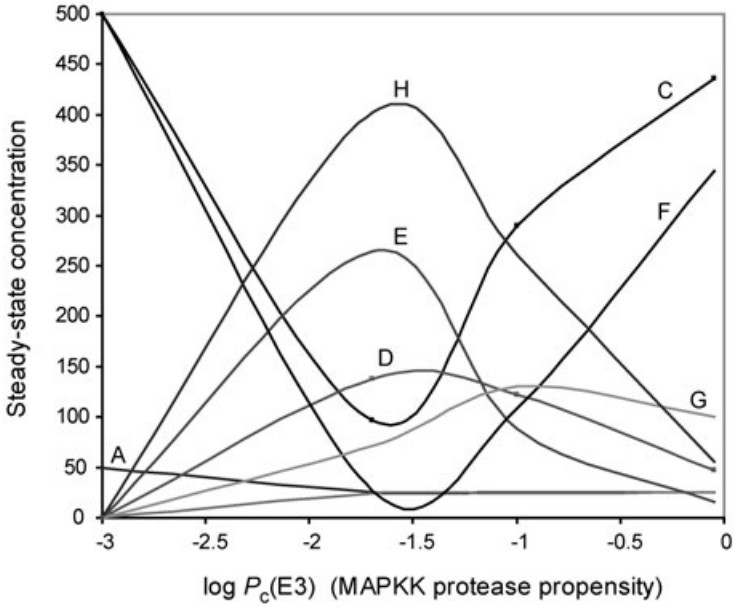

Fig. 3. *Influence of the MAPKK-protease efficiency* (P(E3)) *on the steady-state concentrations of different MAPK cascade species* (for abbreviations, see *Table 1*). Model parameters: enzyme efficiencies P_c (E1) = P_c (E2) = P_c (E4) = 0.1, substrates initial concentration: $[A]_0 = 50$, $[C]_0 = [F]_0 = 500$. The maximum amplification of cascade signal (the maximum concentration of H) at these conditions is obtained for enzyme E3 efficiency within the range of P_c(E3) = 0.01 – 0.02. Similar ranges are obtained for the optimal efficiency of enzymes E2 and E4 (not shown).

observed in studies based on numerical solutions of the kinetics differential equations [9][12]. The potential for downgrading or upgrading the products and substrates concentrations by inhibiting the corresponding enzymes is illustrated in *Table 3*.

Table 2. *Effects of Modeling Enzyme Inhibition in the MAPK Cascade by Decreasing the Variable Enzyme Efficiency from 0.5 to 0.02*. The other three efficiencies equal to 0.1 were kept constant, at initial concentrations of MAPKKK, MAPKK, and MAPK equal to 50, 500, and 500, resp.

Enzyme	Species	Concentration change	Change [%]
E1	MAPK-PP	330 → 100	− 70
	MAPKK-PP	140 → 25	− 82
	MAPKK	220 → 400	+ 82
	MAPK	60 → 230	+ 383
E2	MAPKK	395 → 210	− 47
	MAPK	260 → 60	− 77
	MAPK-P	140 → 340	+ 243
E3	MAPKK	420 → 95	− 77
	MAPK	300 → 25	− 92
	MAPK-PP	80 → 400	+ 500
E4	MAPK-PP	100 → 430	+ 430
	MAPK	290 → 10	− 97

Table 3. *Inhibiting Enzymes E1 to E4 as a Tool for Controling the MAPK Pathway*

Objective	Action	Validity range
Decrease [MAPK]	Inhibit E2, E3, E4	$P = 0.9 \rightarrow 0.02$
Increase [MAPK]	Inhibit E1	$P = 0.9 \rightarrow 0$
Decrease [MAPK-PP]	Inhibit E1	$P = 0.9 \rightarrow 0$
Increase [MAPK-PP]	Inhibit E3, E4	$P = 0.9 \rightarrow 0.02$
Decrease [MAPKK]	Inhibit E3	$P = 0.9 \rightarrow 0.02$
Increase [MAPKK]	Inhibit E1	$P = 0.9 \rightarrow 0$

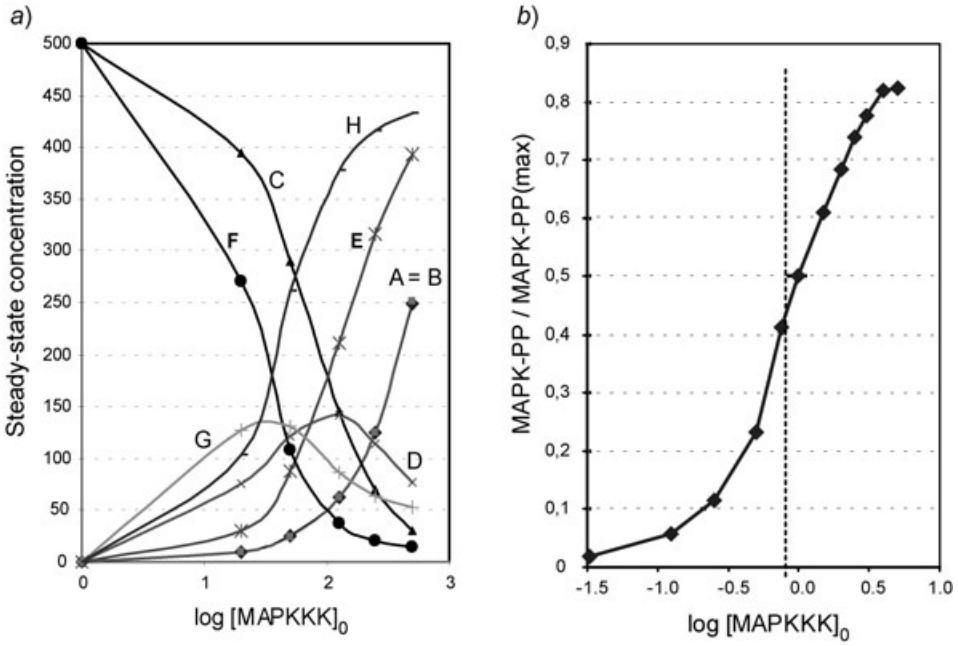

Fig. 4. a) *Semi-logarithmic plot of the steady-state concentrations of substrates' and products' dependence on the initial concentration of MAPKKK in MAPK cascade* (for abbreviations, see *Table 1*). Model parameters: transitional probabilities $P_c(E1) = P_c(E2) = P_c(E3) = P_c$ (E4) = 0.1; initial concentrations $[C]_0 = [F]_0 = 500$. b) *Predicted relative stimulus/response curve for MAPK-PP with input stimulus* (the MAPKKK initial concentration) *expressed in multiples of* EC_{50}. The slope of the MAPK-PP curves in both figures evidences for the significant cascade-signal amplification.

More generally, these analyses indicate the potential of the CA modeling of the patterns of down- and up-regulation of cellular pathways. This might contribute to the design of drugs with reduced side effects by selecting as drug candidates the species whose inhibition is expected to have the least effect on the other molecules. Thus, a drug designed to decrease [MAPK] in the analyzed system would best be an E2 enzyme inhibitor.

4.2. *Varying the Concentration of MAPKKK at Constant Enzyme Efficiencies.* Another line of analysis is to study how the variation in the initial concentration of MAPKKK, which is the major downstream effector, affects the MAPK cascade, when

keeping the enzyme activity constant. *Fig. 4*, *a* shows the dynamics of the concentrations of all substrates and products for a 25-fold increase of $[MAPKKK]_0$ from 20 to 500 cells, as well as at constant efficiencies of E1 to E4 ($P(E) = 0.1$), and at constant initial concentrations of MAPKK and MAPK equal to 500 cells. In the semilogarithmic plot of *Fig. 4*, *a*, the MAPK-PP and MAPKK-PP ascending curves are sigmoidal, as are the descending curves of the respective substrates MAPK and MAPKK, respectively. The sigmoidal pattern is also manifested in *Fig. 4*, *b*, with the predicted stimulus/response MAPK-PP curve in semilogarithmic plot, the input stimulus in which is expressed in multiples of EC_{50}, *i.e.*, the concentration of MAPKKK that produces 50% maximal response. This behavior is typical for alosteric enzymes that do not obey *Michaelis – Menten* kinetics, and, thus, evidences for a cooperative effect of cascade enzymes. Our finding confirms the result of *Huang* and *Ferell* [9], obtained by numerically solving the differential rate quations, where the concentration of E1 was selected as a basic variable.

4.3. *Simultaneous Variation of MAPKKK Concentration and Enzymes Competence.* The dynamics of the MAPK cascade signaling pathway can be analyzed in more detail with simultaneous variation of substrate concentrations and enzyme efficiencies,

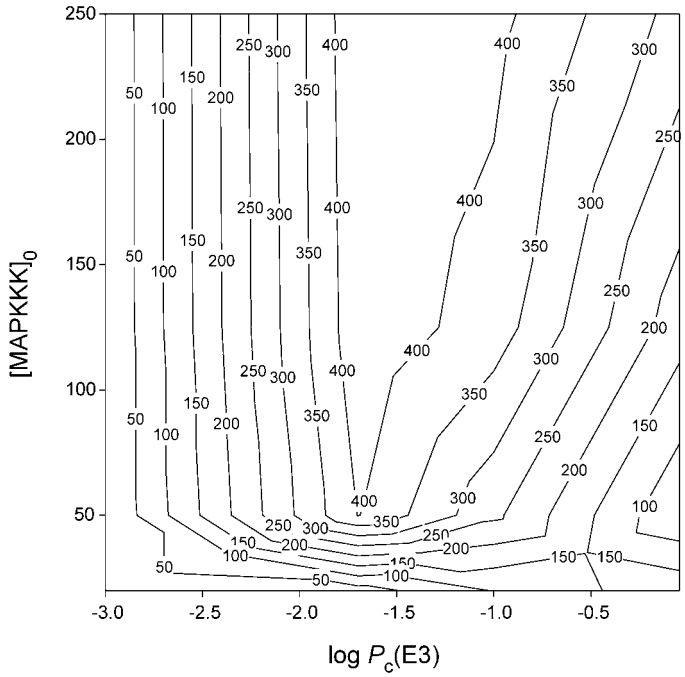

Fig. 5. *Contour plot of the MAPK-PP steady-state concentration at variable MAPKKK initial concentration and variable MAPKK-protease efficiency.* Model parameters: enzyme efficiencies $P_c(E1) = P_c(E2) = P_c(E4) = 0.1$; initial concentrations $[MAPKK]_0 = [MAPK]_0 = 500$. The plot shows that the optimal condition for obtaining the highest MAPK-PP contour level of 400 cells is arrived at $P_c(E3) \geq 0.02$. Within this range of probability values, the cascade-signal amplification, as assessed from the MAPK-PP contour lines, increases with the increase in the initial stimulus (MAPKKK initial concentration). At a constant MAPKKK value higher than 50 cells, the signal amplification passes through a maximum, as was shown in detail in *Fig. 3*.

expressing the results in contour plots (*Fig. 5*). We varied [MAPKKK] within a 25-fold range (20, 50, 125, 250, 500 cells), keeping [MAPKK] and [MAPK] at a constant level of 500 cells. The variable enzyme efficiency was studied within the 900-fold range from 0.001 to 0.9, keeping the other enzymes efficiencies at a level of 0.1. We have performed only a few calculations with $P_c = 0.001$, because the results have shown that the steady-state concentrations are very close to the initial parameter values. Thus, with initial concentrations of MAPKKK, MAPKK, and MAPK equal to 50, 500 and 500 cells, respectively, we have obtained, after 5000 iterations for 50 runs, the following average values: 49.5 ± 0.6, 493.6 ± 5.4, and 486.1 ± 14.3, respectively. In the remaining trials, we approximated the results for $P_c = 0.001$ to the initial parameter values.

Varying $[MAPKKK]_0$ and E1 efficiency (not shown) did not provide surprising results, because both variables increase the yield of reaction products. Yet, the CA models showed a pattern of dominance of the concentration of substrate A over E_1 efficiency. Thus, at $[MAPKKK]_0 = 20$ cells, the 45-fold increase in E1 activity from 0.02 to 0.90 results in only approximately a 4.5-fold increase in the MAPK → MAPK-PP conversion ratio. In contrast, even at relatively low activity of E1 ($P_c = 0.02$), the increase of $[MAPKKK]_0$ from 20 to 250 (12.5-fold) increases the production of MAPK-PP from 50 to 350 (7-fold; *Fig. 6*).

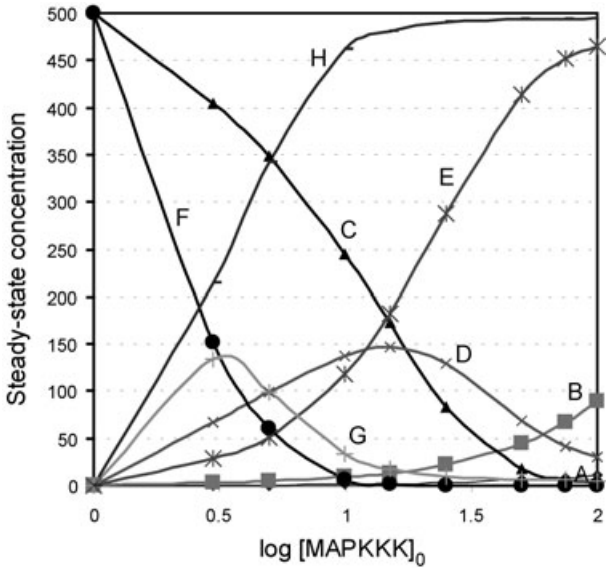

Fig. 6. *Semi-logarithmic plot of the steady-state concentrations of substrates and products in the MAPK signaling cascade* vs. *initial concentration of MAPKKK* (for abbreviations, see *Table 1*). Model-optimized parameters: enzyme efficiencies: $P_c(E1) = 0.1$, $P_c(E2) = P_c(E3) = P_c(E4) = 0.02$; initial concentrations $[C]_0 = [F]_0 = 500$ cells. At the very low MAPKKK initial concentration of only 10 cells, 93% of the dose maximum response is reached.

The variation of the activities of enzymes E2, E3, and E4 produces contour plots with interesting features. This is illustrated for enzyme E3 in *Fig. 5*, where the contour lines show levels of constant steady-state concentration of MAPK-PP (the level of the cascade-output signal). The enzyme effect on the yield of MAPK-PP passes through a

maximum at P_c (E3) = 0.02 to 0.1. The decrease in the MAPK-PP production is expected when E3 becomes more active, because this enzyme reduces the concentration of MAPKK-PP, which catalyzes MAPK phosphorylation. However, the increase in the MAPK-PP concentration within the P_c(E3) range of 0.001 to 0.02 of enzyme activity, for the broad range of [MAPKKK] $\geq$ 25 cells, is a trend that hardly could be anticipated. One can derive from the contour plots the information that suppressing the activity of E2, E3, and E4 enzymes to a level obtained at a transition probability P_c of 0.01 to 0.02, would enable reaching 80% of the maximum MAPK-PP concentration at relatively low concentrations of MAPKKK. A further maximization of the MAPK-PP signal could result from a more-favorable combination of the four enzyme efficiencies, namely, a high one for enzyme E1, and low ones for enzymes E2, E3, and E4, as follows from the patterns described above. Such a combination is, *e.g.*, P_c (E1) = 0.1, P_c (E2) = P_c (E3) = P_c (E4) = 0.02 (see *Fig. 6*). Conversely, a substantial inhibition of these enzymes (*e.g.*, at $P_c \gg 0.02$) would minimize the cascade-signal amplification.

Concluding our analysis, we would like to emphasize that although we reproduced in our study the main results of the *Huang–Ferell* differential-equation model [9] concerning the cascade-signal amplification and the enzymes alosteric effect, the CA modeling of the MAPK cascade pathway reported here was not aimed at exact reproduction of previous work. Rather, it was aimed to demonstrate the potential of the CA method to model basic patterns in pathways of interest, and to indicate the ways to control the pathway dynamics by selective enzyme inhibition and concentration variation. Work is in progress to extend this methodology to larger networks.

We thank Dr. *C.-K. Cheng*, VCU, for technical assistance with the cellular automata program, and Dr. *D. L. Peterson*, VCU, for helpful discussions. *D. B.* acknowledges support from *NIH* (grant No. 5-22405).

REFERENCES

[1] S. Wolfram, 'A New Kind of Science', Wolfram Media, Champaign, IL, 2002.
[2] A. Neuforth, P. G. Seybold, L. B. Kier, C. K. Cheng, *Int. J. Chem. Kinet.* **2000**, *32*, 529.
[3] D. Bonchev, in 'Handbook of Proteomics Methods'. Ed. M. Conn, Humana, New York, 2003, p. 451.
[4] L. B. Kier, C. K. Cheng, B. Testa, P. A. Carrupt, *J. Mol. Graphics* **1996**, *14*, 227.
[5] L. B. Kier, C. K. Cheng, *J. Mol. Graphics* **2000**, *18*, 29.
[6] J. R. Weimar, in 'Cellular Automata', Eds. S. Bandini, M. Tomasini, B. Chopard, Springer, Berlin, 2002, p. 294.
[7] T. Toffoli, *Physica D* **1984**, *10*, 117.
[8] R. Lumry, R. B. Gregory, in 'The Fluctuating Enzyme', Ed. G. R. Welch, Wiley-Interscience, New York, 1986.
[9] C.-Y. F. Huang, J. E. Ferell, *Proc. Natl. Acad. Sci. USA* **1996**, *93*, 10078.
[10] U. S. Bhalla, R. Iyengar, *Science* **1999**, *283*, 381.
[11] B. N. Kholodenko, *Eur. J. Biochem.* **2000**, *267*, 1583.
[12] F. A. Brightman, D. A. Fell, *FEBS Lett.* **2000**, *482*, 169.
[13] T. S. Shimizu, D. Bray, in 'Foundations of Systems Biology', Ed. H. Kitano, MIT Press, Cambridge, MA, 2001, p. 213.
[14] B. Schoeberl, C. Eichler-Jonsson, E. D. Gilles, G. Müller, *Nat. Biotechnol.* **2002**, *20*, 370.
[15] M. Hatakeyama, S. Kimura, T. Naka T. Kawasaki, N. Yumoto, M. Ichikawa, J.-H. Kim, K. Saito, M. Saeki, M. Shirouzu, S. Yokoyama, A. Konagaya, *Biochem. J.* **2003**, *373*, 451.
[16] T. S. Shimizu, S. V. Aksenov, D. Bray, *J. Mol. Biol*. **2003**, *329*, 291.

Received September 27, 2004